# Time domain simulation of the unidirectional and directional focused waves

**B.B. Zhao[a], Y. Xu[a], K. Zheng[a], W.Y. Duan[a], Y.L. Shao[a,b], R.C. Ertekin[a,c]**

a. College of Shipbuilding Engineering, Harbin Engineering University, Harbin, China
b. Department of Mechanical Engineering, Technical University of Denmark, Lyngby, Denmark
c. Department of Ocean and Resources Engineering, University of Hawaii, Honolulu, USA
Email: zhengkunpaul@hrbeu.edu.cn

## HIGHLIGHTS:

- Simulations of a focused wave by High-Level Irrotational Green-Naghdi (HLIGN) equations and Harmonic Polynomial Cell (HPC) method is compared for the first time.
- In the unidirectional focused wave simulation, the water depth effect for the wave kinematics and wave profile is considered.
- The directional effect is considered in the simulation of directional focused wave.

## 1 INTRODUCTION

The phase focusing is considered to be a significant mechanism for the formation of "short-lived" extreme waves, and this attracts many experimental and numerical investigations.

Laboratory studies were carefully performed to provide a benchmark to investigate the focused waves (Baldock et al., 1996; Johannessen and Swan, 2001; Grue and Jensen, 2006). Among that, Baldock et al. (1996) is widely used as the benchmark of the two dimensional focused wave in deep water. And Johannessen and Swan (2001) is another benchmark for the experimental 3-D focused wave. It is still attractive to develop an accurate and efficient wave model to investigate the focused wave.

In order to satisfy this demand, the High-Level Irrotational Green-Naghdi (HLIGN) equations derived by Kim et al. (2001) are utilized in this investigation. As the name indicates, the HLIGN equations are categorized into different levels. The higher level IGN equations are more accurate (Zhao et al., 2015) as shown before.

The Harmonic Polynomial Cell (HPC) method is applied for further verification of the HLIGN results. The HPC method is originally derived by Shao and Faltinsen (2012, 2014). The comparison with other potential solvers shows that the HPC method has good accuracy and efficiency.

The theoretical framework of the HLIGN equations and the HPC method is briefly described Sections 2 and 3, respectively. The numerical cases including the 2D and 3D focused wave as well the effects of water depth and directions are presented in Section 4. Summaries and conclusions of this study are provided in Section 5.

## 2 THE HLIGN EQUATIONS

The fluid is assumed to be incompressible and inviscid and the flow is irrotational. The HLIGN equations are briefly introduced in two dimensions. The velocity field ($u$, $w$) can be expressed by the stream function $\psi(x, z; t)$ as follows. The stream function is expressed by a series of polynomials with stream function coefficients $\psi_n$.

$$u(x,z,t)=\frac{\partial \psi(x,z;t)}{\partial z}, \quad w(x,z,t)=-\frac{\partial \psi(x,z;t)}{\partial x}, \tag{1}$$

$$\psi(x,z;t)=\sum_{n=1}^{K}\psi_n(x;t)f_n(\gamma), \quad f_n(\gamma)=\left[(z+d)/(\eta+d)\right]^{2n-1}, \tag{2}$$

where $K$ is the level of the HLIGN model, $\eta$ is the free surface elevation and the water depth is $d(x)$. This approximation on wave kinematics could be raised to a higher level by increasing the order of the polynomials $K$. The corresponding HLIGN equations are written as IGN-K, such as IGN-5. The higher level IGN equations are strongly nonlinear and strongly dispersive wave models (Duan et al., 2017).

Following Hamilton's principle, the HLIGN equations (Kim et al., 2001; Zhao et al., 2015) are given by the three equations below.

$$\frac{\partial \eta}{\partial t}+\frac{\partial \hat{\psi}}{\partial x}=0, \quad (z=\eta), \tag{3a}$$

$$\frac{\partial \hat{\phi}}{\partial t}+\frac{\partial}{\partial x}\frac{\partial E_k}{\partial \eta_{,x}}-\frac{\partial E_k}{\partial \eta}+g\eta=0, \tag{3b}$$

$$f_n(1)\frac{\partial \hat{\phi}}{\partial x}+\frac{\partial}{\partial x}\frac{\partial E_k}{\partial \psi_{n,x}}-\frac{\partial E_k}{\partial \psi_n}=0, \tag{3c}$$

where $\hat{\phi}$ and $\hat{\psi}$ represent the velocity potential and the stream function on the surface, respectively. The $\eta_{,x}$ and $\psi_{n,x}$ are the spatial derivatives of the free surface and the stream function coefficients, respectively. $E_k$ represents the

kinematic energy. For further explanations on the HLIGN equations, the reader is referred to Zhao et al. (2015).

# 3 THE HPC METHOD

As in the HLIGN equations, the two-dimensional flow field is assumed to be incompressible, inviscid and irrotational. The flow field could be governed by the Laplace equation. The Mixed Eulerian-Lagrangian method is adopted to make the free-surface elevation satisfy the fully nonlinear free-surface condition. If the flow field is discretized by quadrilateral cells, the local Cartesian coordinates could be established at the central 9$^{th}$ node with 8 boundary nodes surrounding it. Then the velocity potential at any location within the cell can be approximated by superposition of 8 harmonic polynomials as follows:

$$\Phi(\tilde{x},\tilde{z})=\sum_{j=1}^{8} b_j F_j(\tilde{x},\tilde{z}), \tag{4}$$

where $\tilde{x}$ and $\tilde{z}$ are the local coordinates relative to the stencil centre. The $b_j$ and $F_j$ are the unknown coefficients of the eight harmonic polynomials (Shao and Faltinsen, 2014).

The harmonic polynomials automatically satisfy the Laplace equation, everywhere. The $b_j$ can be determined through a boundary-value problem. The velocity potential is then expressed by the eight boundary velocity potentials $\Phi_i(\tilde{x},\tilde{z})$:

$$\Phi(\tilde{x},\tilde{z})=\sum_{i=1}^{8}\left[\sum_{j=1}^{8} c_{j,i} F_j(\tilde{x},\tilde{z})\right]\Phi_i, \tag{5}$$

where the $c_{j,i}$ is the elements of the inverse of the harmonic polynomial matrix.

The $F_j$ ($j$ =2, 3, …, 8) equals to zero considering the coordinates of the central node is (0,0). Therefore, the velocity potential on the 9$^{th}$ central node is specified as the linear combination of the surrounding velocity potentials:

$$\Phi_9=\sum_{i=1}^{8} c_{1,i}\Phi_i. \tag{6}$$

In each cell, this expression is enforced on each central node which is then be used as the boundary node of a neighboring cell.

# 4 TEST CASES

## 4.1 UNIDIRECTIONAL FOCUSED WAVE

Baldock et al. (1996) performed an experimental study on the unidirectional focused wave in intermediate water depth. We reproduced these focused waves by using the HLIGN equations. The focused waves are also simulated when $d$ =1.4 and 2.1m, to investigate the influence of water depth.

To be consistent with the experiment, the wave flume is 20m long, and 0.7m deep in our numerical study. The equally spaced period range of focused wave groups is [0.6s, 1.4s]. The input amplitude $A$ =29$a_i$ is set to 52 mm to obtain the same crest elevation for the numerical and experimental focused wave. The theoretical focal position and focal time are specified as $x_f$ =8.0m and $t_f$ =20s, respectively. The convergence study, including the grid size, the time step and the levels, is performed in each simulation. The time history and velocity profile of the focused wave are displayed in Fig. 1.

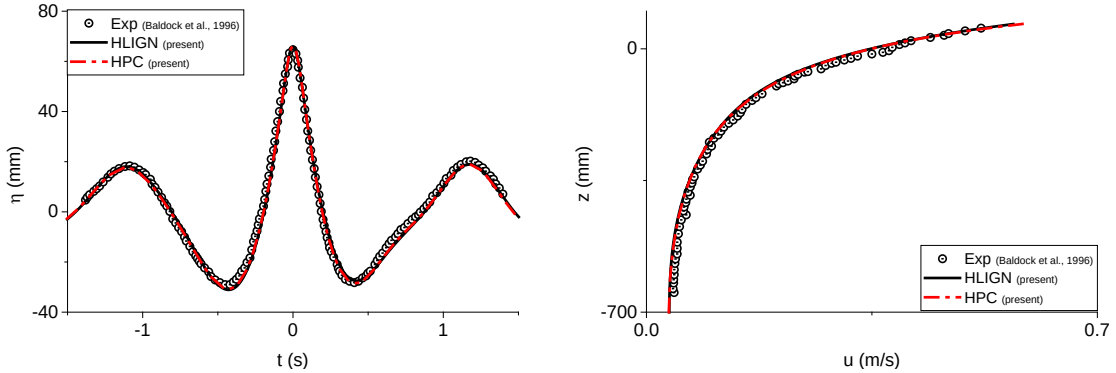


**(a) *Time history at focal location*** **(b) *Horizontal velocity beneath the focused crest***

**Fig.1 Unidirectional focused wave in intermediate water depth ($d$ =0.7m)**

Both the HLIGN and the HPC numerical surface elevations agree well with the experimental data obtained from Baldock et al. (1996). It is shown that the HLIGN equations are as accurate as the fully nonlinear HPC method, considering the HPC is a highly accurate field solver (Shao and Faltinsen, 2012).

The relationship between the input amplitudes and the exact focal position, measured from ($x_f$, $t_f$), is presented in Fig. 2. Good agreement is achieved between the HLIGN and HPC numerical results. The numerical results can well predict the downstream shift of the exact focal location which has also been observed by Baldock et al. (1996).

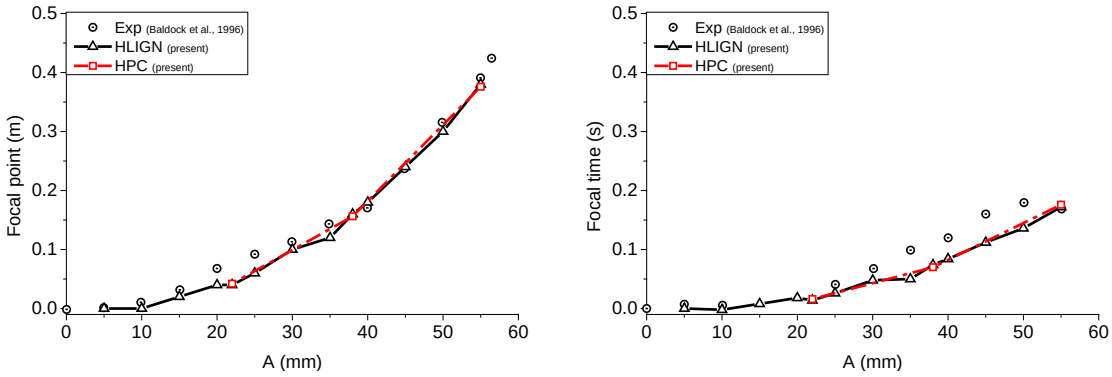


**(a) *Position of the focal point*** **(b) *Time of focusing (at focal position)***

**Fig.2 Relationship among the input amplitude, the focal position and the focal time (*d* =0.7m)**

The focused waves are also simulated for different water depths, d =0.35, 0.7, 1.4 and 2.1m, in Fig. 3. To focus our attention on the effect of water depth, the numerical focused crest elevation is precisely specified as 55mm by carefully optimizing the input amplitudes.

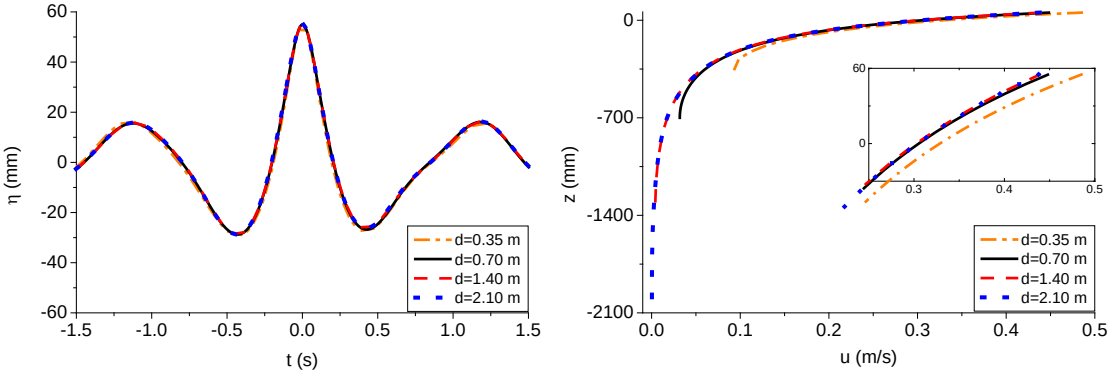


**(a) *Time history at focal location*** **(b) *Horizontal velocity beneath the focused crest***

**Fig.3 Unidirectional focused wave in different water depth (*d* =0.35, 0.7, 1.4 and 2.1m)**

Even though we specified the crest elevation, the profile of the focused wave is not constrained. It is shown that the focused wave profile is the same for different water depths although the nonlinearity is strong. The effects of water depth on the surface elevation are not obvious. The horizontal velocity beneath the focused crest is shown in Fig. 3(b). In order to show the difference more clearly, the detailed view of the velocity closed to the focused crest is displayed as a sub-figure. It is shown that the water depth affects the wave kinematics significantly, even though the focused crest elevation is specified for different water depths. It is quite clear that the horizontal velocity does not decrease to zero if *d* equals to 0.35 and 0.7 m. These focused waves for *d* =1.4 and 2.1m can be regarded as in deep water. The reduction of the water depth increases the horizontal velocity at the focused crest. The velocity for *d* =0.35m is significantly larger than that for the other water depth.

### 4.2 DIRECTIONAL FOCUSED WAVE

Johannessen and Swan (2001) conducted another laboratory study on the 3D focused wave. The influences of the input amplitude and directionality of the wave field are considered in their experiments. To be consistent with their experiments, the numerical wave flume is set to 15m long, 25m long, and 1.2m deep in the simulations. The period range of the focused wave groups is also [0.6s, 1.4s]. The input amplitude *A* is 55mm. However, there are 61 wave components which have 91 directions for each frequency component. The theoretical focal position is specified as ($x_f$, $y_f$) =(5.5, 12.5)m. The directional spreading parameter *s* is chosen as 4 (strongly spreading) and 45 (weakly spreading). The snapshot and the time history of the directional focused wave are displayed in Fig. 4.

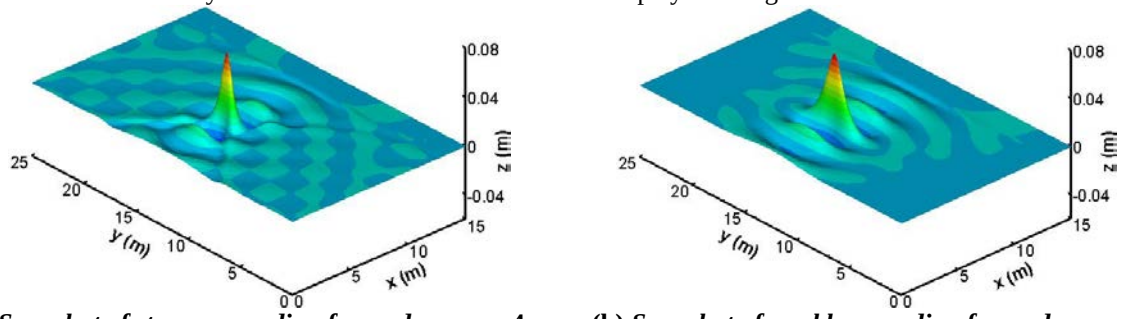


**(a) *Snapshot of strong spreading focused wave, s*=4** **(b) *Snapshot of weakly spreading focused wave, s*=45**

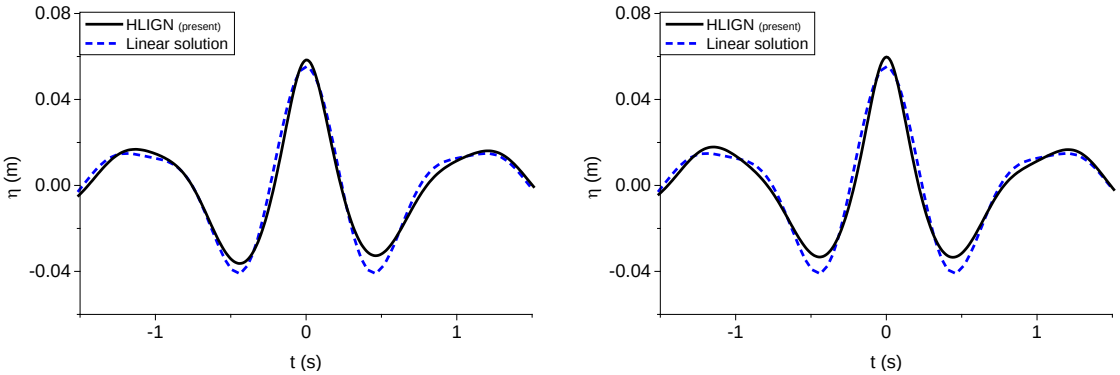


**(c) *Time history of strong spreading focused wave, s*=4 (d) *Time history of weakly spreading focused wave, s*=45**
**Fig.4 Directional focused wave (*d* =1.2m)**

Despite there is no laboratory data available for these two focused waves, the directional effect is distinct between the strongly spreading and the weakly spreading focused waves. And the nonlinear focused crest obtained by the HLIGN simulations is steeper and higher than the linear solutions (superposition of the Airy waves).

**More test cases including the 2D and the 3D focused waves will be compared with the experimental data and presented at the workshop.**

## 5 CONCLUSIONS

The strongly nonlinear HLIGN equations and the HPC method are utilized here to simulate the focused waves in intermediate water depth as well as in deep water. The HLIGN free surface and wave kinematics are compared with the well-accepted laboratory data and the results of the HPC method. It is demonstrated that both the HLIGN equations and the HPC method can accurately simulate the surface elevation and particle velocity of focused waves. And both of these models can simulate the cases in a couple of minutes.

The effect of water depth on focused waves is also carried out in two dimensions. It provides a new perspective on the investigation of the focused wave kinematics. For the focused waves with the same crest elevations in different water depths, the velocity distribution is significantly distinct but the wave profiles are the same. The reduction of the water depth increases the horizontal velocity at the focused crest.

The directional effect is considered in the simulation of directional focused wave. And the nonlinear focused wave is obviously different from the linear solutions.

## ACKNOWLEDGMENTS

The first and fourth authors' (B.B. Zhao and W.Y. Duan) work is supported by the National Natural Science Foundation of China (Nos. 11772099, 51679043, 11972126), the Heilongjiang Touyan Innovation team Program and the special Fund for Basic Scientific Research of Central Colleges (Harbin Engineering University). The third author (K. Zheng) is supported by Ph.D. Student Research and Innovation Fund of the Fundamental Research Funds for the Central Universities (3072019GIP0101).

## REFERENCES

[1] Baldock, T.E., Swan, C. & Taylor, P.H. (1996), `A laboratory study of nonlinear surface waves on water', Philosophical Transactions of the Royal Society Series A. 354(1707), 649-676.

[2] Duan, W.Y., Zheng, K., Zhao, B.B. & Ertekin, R.C. (2017), `Steady solutions of high-level Irrotational Green-Naghdi equations for strongly nonlinear periodic waves', Wave Motion 72, 303-316.

[3] Grue, J. & Jensen, A. (2006), `Experimental velocities and accelerations in very steep wave events in deep water', European Journal of Mechanics-B/Fluids 25(5), 554-564.

[4] Johannessen, T. & Swan, C. (2001), `A laboratory study of the focusing of transient and directionally spread surface water waves', Proceedings of the Royal Society Series A. 457(2008), 971-1006.

[5] Kim, J.W., Bai, K.J., Ertekin, R.C. & Webster, W.C. (2001), `A derivation of the Green-Naghdi equations for irrotational flows', Journal of Engineering Mathematics 40(1), 17-42.

[6] Shao, Y.L. & Faltinsen, O.M. (2012), Towards efficient fully-nonlinear potential-flow solvers in marine hydrodynamics, in `ASME 2012 31st International Conference on Ocean, Offshore and Arctic Engineering', American Society of Mechanical Engineers, 369-380.

[7] Shao, Y.L. & Faltinsen, O.M. (2014), `A harmonic polynomial cell (HPC) method for 3D Laplace equation with application in marine hydrodynamics', Journal of Computational Physics 274, 312-332.

[8] Zhao, B.B., Ertekin, R. C. & Duan, W.Y. (2015), `A comparative study of diffraction of shallow-water waves by high-level IGN and GN equations', Journal of Computational Physics 283, 129-147.